On the mechanical role of intra-articular pressurization in damaged human joints

Vitucci, Gennaro; De Tommasi, Domenico; Mishuris, Gennady

Published in:
European Journal of Mechanics - A/Solids

DOI:
10.1016/j.euromechsol.2022.104866

Publication date:
2023

Citation for published version (APA):
Vitucci, G., De Tommasi, D., & Mishuris, G. (2023). On the mechanical role of intra-articular pressurization in damaged human joints. *European Journal of Mechanics - A/Solids*, *100*, Article 104866. https://doi.org/10.1016/j.euromechsol.2022.104866

On the mechanical role of intra-articular pressurization in damaged human joints

Gennaro Vitucci[a,*], Domenico De Tommasi[a], Gennady Mishuris[b]

[a]*Department of Civil, Environmental, Land, Building Engineering and Chemistry (DICATECh), Polytechnic of Bari, Italy*
[b]*Department of Mathematics, Aberystwyth University, United Kingdom*

Abstract

A large part of world population suffers of degenerative pathologies deriving from the degradation of articular cartilage. It is well established the concurrence to this of synovial disorders, such as inflammation and stiffening, which are sometimes seen as precursors of further cartilage damage. The precise relation of causality between the two phenomena is however still unclear. Whereas proposed models describe which study the mechanical response of cartilage, they usually neglect the impact of synovial fluid pressurization, considering it as a secondary effect. However, such an assumption may not be always valid, especially in case of deteriorated mechanical properties of the cartilage, such as in arthritis of various kinds. In this paper, we estimate the load-bearing capacity of the whole synovial capsule and its impact to the process. We consider a fluid-solid interaction of the cartilage, intra-articular fluid and synovial membrane by extending a well-known mathematical model of biphasic tissue. Our results show that there is a possible previously neglected beneficial effect arising from the fluid pressurization, particularly important in case of deteriorated cartilage mechanical properties.

Keywords: synovial joint, damaged cartilage, synovial fluid, intra-articular pressure, synovial membrane

1. Introduction

The function of the joint capsule, i.e. the compartment in which animal articulation consists, is manifold and the scientific community is open to debate about some of the related medical issues. Doubtlessly, it helps, both actively and passively, to keep the joint in place and provides stability by not permitting the conjoining bones to slip over each other out of the dedicated surfaces (a review in Ralphs and Benjamin [36]).

One of the components of synovial joints, and perhaps the most extensively investigated, is articular cartilage. Its surface is wet with an external fluid which completely fills the synovial cavity. This must be kept inside by the capsule shell, which is composed of an inner impermeable layer, the synovial membrane, covered by a fibrocartilagineous, stiffer outer layer. These two are attached to the bones at their extremities and form a deformable wall which inflates and deflates depending on the position of the contact across the articular cartilage surface, i.e. according to the loading and range of extension of the limb. Additional components such as menisci and ligaments can also be present.

Many kinds of articular disturbs, especially osteo- or rheumatoid arthritis but also post-traumatic ones, arise in conjunction with synovitis, an inflammation of the membrane, and joint effusion, characterized by extra fluid in the cavity. A typical symptom is swollen joints. The synovial fluid is known to enhance lubrication and to be the mean for transporting nutrients to cartilage and dead cells out of it. On the other hand, it may have a key role in assisting the transmission of loads outside the contact area. Whether this is the case or not, it has been debated in the past. It has been regularly observed that diseased joints show higher intra-articular pressures than healthy ones. The phenomenon is even sharpened during flexion (see Jayson and Dixon [22, 21], Jawed et al. [20], Viitanen et al. [45]). Myers and Palmer [32] revealed *in vivo* that diseased joints inflate more difficultly than intact ones. The intra-articular pressure soars more than linearly with liquid volume injected into the cavity.

Experimentalists, for exploring this occurrence, have started to try and pump fluid into the capsule and to measure the resulting pressure-volume curves, whose derivative is called elastance or compliance depending on the axes order. The tests where performed *in vitro* on cadaveric samples. Various measurements have been carried out at different ranges of flexion (Nade and Newbold [33], Schwarz et al. [39], Yen et al. [54]).

Effusions cause also loss of strength and control in the surrounding muscles because of neuronal inhibition (Fahrer et al. [9], Torry et al. [44], Hopkins et al. [18]). Volume of effusion, intra-articular pressure and muscles inhibition seem to be all linearly dependent (Spencer et al. [42]). The swollen capsule impedes a correct blood circulation in the tissues surrounding it too [13]. It might be that muscles inhibition is beneficial in mitigating the pain and solicitations to diseased joints. We wonder which, if any, is the mechanical advantage of effusions in the context of contact.

*Corresponding author
Email address: gennaro.vitucci@poliba.it (Gennaro Vitucci)

In hips and shoulders, the most mobile joints of the body, the fluid is maintained by a seal structure called labrum, a ring which sits on the acetabulum, the socket of the bone. Labral tears often accompany the arthrodial pathologies. The tears constitute a passage for the intra-articular fluid which leaves the contact area. Contrary to the synovial membrane, this seal has received some attention from mechanical modellers. Some authors, such as Henak et al. [16], Todd et al. [43], have published a very detailed finite element analysis, including nonlinearities in the mechanical properties of cartilage and labrum. The in vitro experiments of Ferguson et al. [12] confirmed the same team's expectation [10, 11] when they focused on variations in global joint consolidation speed. The labrum impermeability gives opportunity to a thin film of synovial fluid to pressurize. Its resistance to be squeezed away evens out the contact pressure. Such a uniformity makes possible to sustain external loads without elevated distortions in the solid, responsible for shear stresses. We try for the first time to have a simplified yet mechanically motivated insight into the most influential factors which coordinate the joint capsule functioning.

In this paper, the cartilage layer is considered biphasic, in the wake of the seminal study by Mow et al. [31]. The contact problem is solved by means of asymptotic analysis. In this field, we refer to the fundamental contributions of Professor Alexander Movchan and Professor Natalia Movchan, to whom this Special Issue is dedicated. The solution procedure of perturbed partial differential equations has been actually systematized in [25]. The method has then been successfully applied by them in a wide spectrum of physical problems, ranging from composites to fracture mechanics, adhesion and biomechanics, just to cite a few (see e.g. [4, 23, 30, 29]). By exploiting the same asymptotics, the contact problem for biphasic cartilage has been repeatedly solved analytically ([3, 1, 2, 46]).

Moreover, the elastic version of Young-Laplace's law is used for the synovial membrane as in [14]. The cavity fluid is trapped in the synovium by the membrane and the cartilage to preserve its volume. Simultaneously, biphasic articular tissue deforms for accommodating an external load. As a first attempt to model the whole capsule, we introduce various simplifications. Chiefly, the cartilage is seen as isotropic and homogeneous, which is not the case in reality (e.g. see our previous works Vitucci et al. [47], Vitucci and Mishuris [46]). Next, in order to obtain closed form analytical expressions for the mass conservation, we explore only a 2D setting. This is though expected to be reasonably accurate along the longest dimension of the contact area, where interstitial fluid flow and rate of contact growth are higher.

Combinations of membrane and cartilage mechanical properties are simulated in order to qualitatively reproduce some of the more common situations for healthy and diseased joints, namely in case of osteoartritis (OA). A previously disregarded role of the intra-articular pressurization seems to suggest alternative mechanical resources of the joint capsule specific anatomical arrangement.

In Section 2 we review an existing asymptotic analysis of biphasic deformation and reduce it to its two-dimensional version. Then we add the contribution of intra-articular pressure and build the mechanical model of the whole capsule. In Section 3 we conduct numerical investigations by exploring the effect of realistic parameters deducted by literature for healthy and OA joints. Finally, in Section 4, we discuss the results, highlight possible implications, available model improvements and suggest meaningful clinical studies.

2. Mechanical model

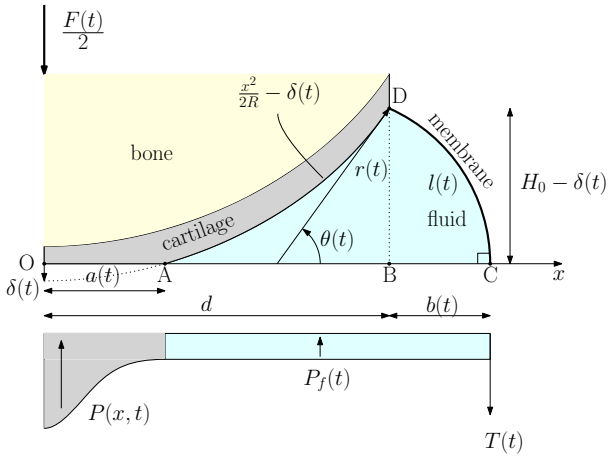

Figure 1: Joint capsule mechanical model. The capsule contains pressurized synovial fluid confined by the articular surface and the synovial membrane. On the bottom line, left to right, the forces of contact, fluid and membrane tension, which oppose the external load. Due to the parabolic shape of the cartilage surface, $H = H_0 - \delta$ with $H_0 = d^2/(2R)$.

In this Section we make use the well-established analysis of biphasic contact developed in [3]. Firstly, we reduce the original three-dimensional model to the two-dimensional subcase and extend it by considering the contribution of an unknown fluid pressure onto the part of cartilage surface which is not in contact. The problem is then coupled to the deformation of the elastic impermeable synovial membrane which completes the capsule mechanical model. This additional relation allows us to retrieve all the sought unknowns.

2.1. 2D biphasic contact with additional synovial pressure

Mixture theory, already developed by Mow et al. [31] with applications on cartilage mechanics, is an effective mathematical framework for modelling multiphasic materials. Following a well established tradition, here we consider cartilage an isotropic homogeneous biphasic tissue. The solid phase elasticity is conferred by a soft proteoglycan matrix reinforced by a collagen network. Equilibrium must be guaranteed to the difference between the solid phase stress and the spherical interstitial fluid pressure.

Simultaneously, the relative fluid velocity depends linearly on the interstitial pressure gradient according to Darcy's law. As a consequence of these assumptions, according to [3, 2], the uni-directional contact of a thin biphasic layer in 2D is written at any time t after the load application as

$$\mathcal{K}\left[\frac{\partial^2 P(x,\cdot)}{\partial x^2}\right](t) = m\left(\frac{x^2}{2R} - \delta(t)\right), \quad x \in [-a(t), a(t)], \tag{1}$$

where the constant m and the integral operator $\mathcal{K}$ account for material thickness and properties (see below for definitions), δ is the contact displacement, $x^2/(2R)$ is a parabola describing the articular surface of curvature radius R, $a(t)$ is the time dependent half-width of the contact, P is the contact pressure.

If everywhere outside the contact zone, including its border, there is a uniform pressure P_f and the only load transferred by contact is represented by a vertical force F_c, then

$$P = P_f(t), \qquad \frac{\partial P}{\partial x} = 0 \qquad \text{for} \quad x = \pm a(t). \tag{2}$$

$$\int_{-a(t)}^{a(t)} P(x,t)\,\mathrm{d}x = F_c(t) \qquad \forall t \geq 0. \tag{3}$$

The integral operator $\mathcal{K}$ and its inverse are defined, see e.g. Argatov and Mishuris [2], as

$$\begin{aligned} \mathcal{K}[Y](t) &= Y(t) + \int_0^t \frac{Y(\gamma)}{\tau}\,\mathrm{d}\gamma, \\ \mathcal{K}^{-1}[Y](t) &= Y(t) - \int_0^t \frac{Y(\gamma)}{\tau} \mathrm{e}^{\frac{\gamma - t}{\tau}}\,\mathrm{d}\gamma, \end{aligned} \tag{4}$$

where the characteristic time τ collects biphasic layer geometry and mechanical properties. Following [2, 3], the parameters of Eqs.(1)-(4) are

$$m = \frac{3E_c}{2h_c^3}, \qquad \tau = \frac{2h_c^2}{3E_c k_c}. \tag{5}$$

The unknowns are the contact pressure $P(x,t)$, the evolution of the contact zone dictated by $a(t)$ and the contact displacement which relates quadratically to a as

$$\delta(t) = \frac{a^2(t)}{6R}. \tag{6}$$

The contact half width a itself is obtained by solving

$$\frac{m}{45R}a^5(t) + \mathcal{K}[a(\cdot)P_f(\cdot)](t) - \frac{\mathcal{K}[F_c](t)}{2} = 0. \tag{7}$$

The previously known solution of [3] is readily obtained by neglecting the second term in the above integral equation. In that special case, a closed form becomes available as

$$a(t) = \left(\frac{45R}{2m}\mathcal{K}[F_c](t)\right)^{1/5}, \tag{8}$$

where the exponent 1/5 substitutes the 1/6 which appeared in the 3D setting. The contact pressure results

$$P(x,t) = P_f(t) + \frac{m}{24R}\mathcal{K}^{-1}\left[\left(a^2(\cdot) - x^2\right)^2\right](t). \tag{9}$$

Consequently, the peak of pressure, i.e. in $x = 0$, is expressed as

$$P_{\text{peak}}(t) = P(0,t) = P_f(t) + \frac{m}{24R}\mathcal{K}^{-1}\left[a^4(\cdot)\right](t), \tag{10}$$

whereas half the overall cartilage contact force becomes

$$\frac{F_c(t)}{2} = \int_0^{a(t)} P(x,t)\,\mathrm{d}x = a(t)P_f(t) + \frac{m}{45R}\mathcal{K}^{-1}\left[a^5(\cdot)\right](t) \tag{11}$$

The formulae Eqs.(6)–(9) are derived in detail in Appendix A.

2.2. Synovial capsule model

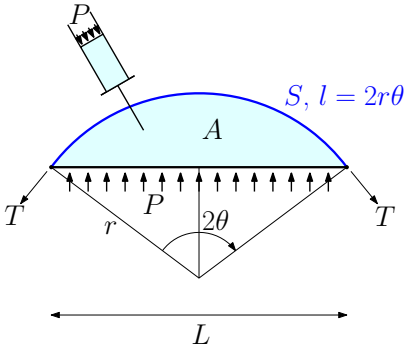

Figure 2: Inflation of an elastic membrane fixed to two extremes. Fluid is injected into the capsule and cannot flow out of it.

We enable the capsule fluid pressurization by means of a linearly elastic synovial membrane, i.e. with no bending stiffness, working as fluid barrier. Its constitutive model is simply stated via its elongation stiffness S as

$$\frac{\mathrm{d}T}{\mathrm{d}l} = \frac{E_m h_m}{l_0} = S, \tag{12}$$

with T and l being its tension and length, E_m and h_m its Young's modulus and thickness. The membrane is anchored to two extremities and it is unstressed. Furthermore, the volume (area in 2D) A of incompressible fluid is contained in the capsule, confined from the other two sides by impermeable constraint and the cartilage layer. The elongation from l_0 to l, which allows the fluid to flow in, induces a synovial pressure P_f (see Fig.2). A balance must be achieved between the pressure contribution $2P_f r\sin\theta$ and the membrane tension $2T\sin\theta$ according to

$$P_f = \frac{T}{r} = S\frac{l - l_0}{r}, \quad l = 2r\theta. \tag{13}$$

It is worth noticing that the latter is a modified Young-Laplace equation, which includes a surface tension changing proportionally with strain.

Besides, the injected volume relates to the system geometry as

$$A = r^2\left(\theta - \frac{\sin 2\theta}{2}\right) = \frac{L^2}{4\sin^2\theta}\left(\theta - \frac{\sin 2\theta}{2}\right). \qquad (14)$$

As a result, the three equations above show the parametric variation of A, P_f and T as functions of the angle θ.

2.3. Fluid-bone interaction in joint capsule

Our aim is to quantify the role of the fluid-filled capsule in sustaining the load $F(t)$ applied to the joint. The fluid is incompressible and we neglect its fluid dynamics, i.e. the pressure $P_f(t)$ is homogeneous.

With the goal of enforcing the fluid incompressibility, we impose that the area A_{ABCD} in Fig. 1 remains constant, i.e. the fluid displaced by the increase of contact area and contact displacement pushes onto the membrane which results in its elongation and stress similarly as in Subsection 2.2. By simple geometric considerations and by assigning the area A_0 occupied by the fluid at every time, including the relation Eq.(6), the mass conservation results into

$$\frac{\phi(\theta)}{d}H^2 + H - \frac{d^2}{4R}\left(2 + \frac{d}{R}\phi_0\right) = 0, \qquad (15)$$

$$\text{with} \quad \phi(\theta) = \frac{\theta - \sin\theta\cos\theta}{2\sin^2\theta}, \quad \phi_0 = \phi(\theta_0). \qquad (16)$$

Notice that Eq.(15) is a quadratic algebraic equation. It allows for explicitly obtaining the height of the membrane hinge $H = H(\theta)$ (see Fig.1) and the contact displacement

$$\delta(\theta) = \frac{a^2(\theta)}{6R} = \frac{d^2}{2R} - H(\theta) \qquad (17)$$

as a capsule constraint enforced via a purely geometric condition described by its relation with the angle θ.

Furthermore, equilibrium has also to be guaranteed (e.g. see the bottom line in Fig. 1). The contribution of the biphasic layer, the fluid and the elastic membrane are on the left-hand side of

$$\frac{F_c}{2} + (d - a + r(1 - \cos\theta))P_f - T = \frac{F}{2}. \qquad (18)$$

If one substitutes the contact law Eq.(11), and the linear elastic Young-Laplace, the balance becomes

$$\frac{m}{45R}\mathcal{K}^{-1}\left[a^5(\theta(\cdot))\right](t) + \left(\frac{d}{r(\theta)} - \cos\theta\right)T(\theta) = \frac{F(t)}{2}, \qquad (19)$$

where Eq.(7) has been used, imposing that the contact pressure at the border of the contact area is the same as in the fluid (details of the derivation in Appendix B).

Summarizing, we have two main equations, mass conservation Eq.(15) and vertical equilibrium (19), plus a set of geometric and constitutive relations which allow to reduce the problem to the search of two functions of time, e.g. $a(t)$ and $\theta(t)$.

Notice that Eq.(19) is a non-linear Volterra integral equation of second kind and we could not shun a numerical approach for its solution. Our alternative endeavor has been borne by transforming it into an ordinary differential equation of unknown θ (details in Appendix B) and solving it in MATLAB® via the library `ode45`, which uses the standard Runge-Kutta method.

3. Results

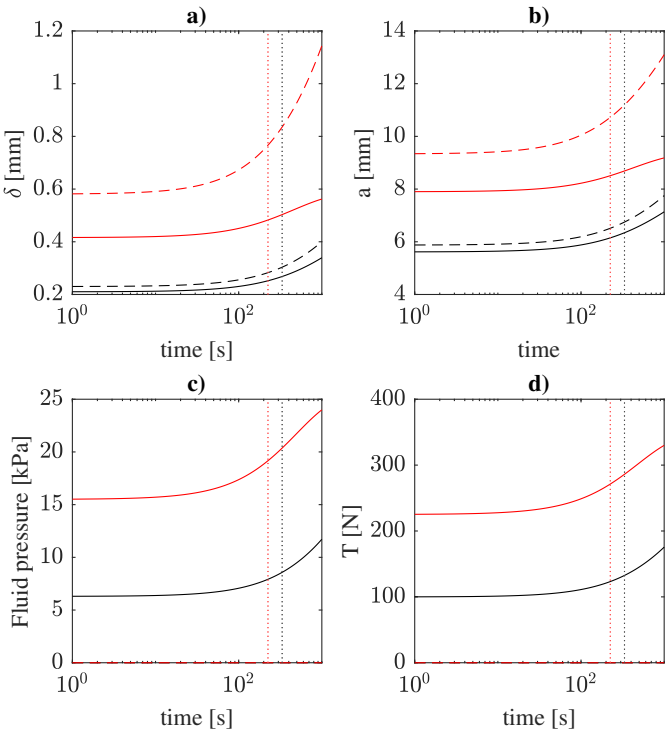

Figure 3: Evolution of main variables under constant load. Black and red stay for healthy and OA cartilage, respectively. Solid and dashed lines indicate whether the synovial membrane is present or not. Vertical lines are placed at $t = \tau$.

Here, according to our model, we explore the implications of the pressurized synovial fluid on a tibiofemural joint mechanical behavior with and without cartilage degradation which might derive from OA.

To this end, we model an articular surface of $R = d = q = 25$mm, where q is the depth in the z-direction perpendicular to the cross section in Fig.1. Notice that the radius choice is in accordance with the minimum curvature radius, the most critical for contact, obtained by us in [46] by analyzing the measurements on medial knee compartments of Hosseini et al. [19].

About cartilage mechanical properties, for healthy joints, we rely on the work of Boschetti et al. [5], who analyzed the real time-dependent deformation behavior of human cartilage in view of biphasic constitutive models. They concluded that the stiffness E_c and permeability k_c are about 0.4MPa and $2 \cdot 10^{-14}\mathrm{m}^4/(\mathrm{N\ s})$, respectively. The tissue thickness is assumed $h_c = 2$mm in line with the

average estimate of Coleman et al. [6] via magnetic resonance. This entails a characteristic time of 333s for a normal cartilage (see definition in Eq.(5)).

Osteoarthritis deteriorates the cartilage. Its prestressed collagen network, which confers it its stiffness, progressively fails. As a consequence, not only E_c decreases, but the layer swells, the interconnected pores of its matrix inflate, thus its permeability dramatically grows. For taking this into account, we rely on the experimental observations by Peters et al. [35], Kleemann et al. [24], Setton et al. [40], Panula et al. [34], Mäkelä et al. [27], Herzog et al. [17]. Compared to normal tissues, we model the effect of OA as a reduction of three times for E_c, an increase of h_c of 50% and a tenfold increase in k_c (summarized in Table 1). This means a reduction of the characteristic time of about one third for the simulated OA versus healthy biphasic tissues.

	d, R, q [mm]	θ_0	k_c [m^4/(N s)]	E_c [MPa]	h_c [mm]	S [kN/mm]
healthy	25	$\pi/4$	$2 \cdot 10^{-14}$	0.4	2	0.58
OA	–	–	$2 \cdot 10^{-13}$	0.4/3	3	–

Table 1: Simulation parameters. Where not specified, the parameter is unchanged between the simulated healthy vs OA cartilage.

To the best of our knowledge, mechanical characterization has not been carried out on the properties of the synovial membrane. Within the scope of this work, we have to settle for reasonable guesses. Looking for example at Wegst and Ashby [50], Moeendarbary and Harris [28], Smith and Wechalekar [41] and considering the membrane to have a Young's modulus in between cartilage and tendons, we assume $E_m = 10E_c$ and of same thickness $h_m = h_c$. Furthermore we assume that the membrane unstressed configuration requires $\delta = 0$ and an angle $\theta_0 = \pi/4$. It is in this way possible to estimate $l_0 = 13.9$mm and the stiffness S of Eq.(12) which thus takes the value of 0.58kN/mm (see again Table 1).

Finally, we simulate the effect of body weight on the response of the 2D medial capsule in the first 1000s from standing. During stance, the human body weight is ideally equally shared by the two knees. Within one knee, the medial compartment is the most loaded and takes 2/3 of half the body weight (see Werner et al. [51], Halder et al. [15]). With an European average body weight of about 700N (Walpole et al. [49]), this results in a constant force on the mediolateral compartment of $F = \frac{700N}{3q}$.

In all the shown results we include four scenarios, which are combinations of two health conditions and the presence or not of the membrane. This latter choice is not only necessary for comparing the findings with literature ones where the membrane is not present, but also have a physiological interest. For healthy joints, indeed, the membrane could work less or close to zero, whereas synovitis, with membrane stiffening and synovial fluid effusion accompany OA disorders.

In Fig.3 the main variables evolution is shown. By looking at Fig.3a)-b) OA tissues deform faster than healthy ones because of their shorter characteristic times. It is clear that the membrane reduces the contact area and displacement. The responsible phenomenon is the capsule pressurization and concomitant elongation of the membrane which becomes increasingly tauter for accommodating the synovial fluid. This is exacerbated greatly in case of deteriorated cartilage layers (see Fig.3c)-d)). We notice a reasonable agreement, at least in terms of order of magnitude, with the in-vivo measurements of synovial fluid pressure by Jawed et al. [20]. The entity of membrane tension does not seem to be any close to the strength of ligaments (e.g. Wegst and Ashby [50]), which means that the functionality of capsule mechanism can be effectively maintained. Nevertheless, the membrane stress might be source of pain and inflammation which are indeed frequent symptoms of articular disorders.

In order to gain more insight into the underlying mechanics, in Fig.4a) we plot the load portion sustained by the contact. For the OA case, only about half of it weigh on the cartilage, whereas the remaining half is directly taken care of by the tension-pressurization resources. This is compared to almost 80% for the healthy joint and 100% in the scenario where the membrane does not work at all. Unsurprisingly, similar considerations can be done about the contact pressure peak evolution in Fig.4b). In this case the membrane inclusion in the model predicts a far higher reduction of pressure peak for the OA case if compared to the healthy one (about 50% vs 15%). One could reasonably argue though that it is not the peak of contact pressure that would damage the cartilage, rather its x-derivatives, which would give origin to shear stresses that cannot be absorbed by the interstitial fluid. For this purpose, in Fig.5 we show the predictions in terms of contact pressure distribution at $t = 0$ and $t = 1000s$. We remark that, also in terms of contact pressure mean slope, the synovial pressurization leads to mechanical advantages and even more so in the case of OA joints. Notice for instance in Fig.5b) that the solid red line is practically flat, which means that the contact pressure is almost the same as the synovial fluid one. Therefore the synovium pressurization allows for a more even allocation of mechanical resources in case the cartilage itself starts to fail.

4. Discussion and conclusions

High intra-articular pressure has been regularly measured in patients affected by articular disorders. We wonder whether it is high pressure which causes cartilage damage or rather a deteriorated articular articular surface which necessitates for an increase in cavity pressure. It has been asked whether we understand enough about capsules mechanics and relation to the body optimum [38].

In order to answer to such a question, we set a two-dimensional problem inside the joint where: the cartilagineous tissue is modelled as biphasic, isotropic and homo-

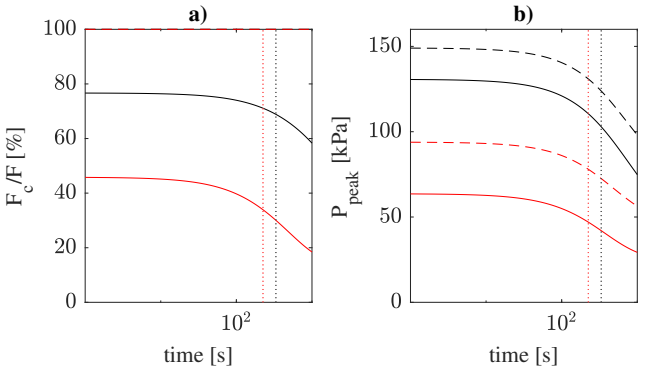

Figure 4: Response of biphasic cartilage under constant load. Black and red stay for healthy and OA cartilage, respectively. Solid and dashed lines indicate whether the synovial membrane is present or not. Vertical lines are placed at $t = \tau$. a) Percentage of load sustained by the cartilage contact. b) Contact pressure peak.

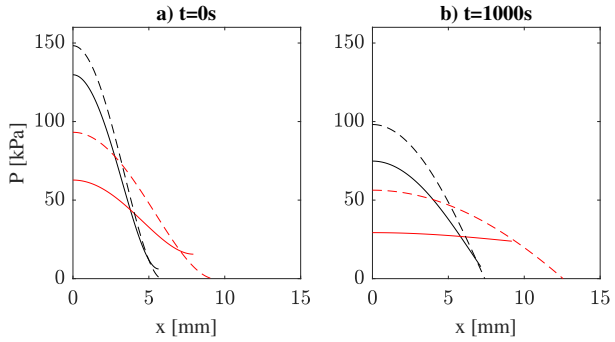

Figure 5: Contact pressure distribution. Black and red stay for healthy and OA cartilage, respectively. Solid and dashed lines indicate whether the synovial membrane is present or not.

geneous; the intra-articular fluid is inviscid; the synovial membrane is impermeable and linearly elastic. The governing equations are mass conservation and equilibrium.

It turns out that, as contact displacement and contact width are univocally related, mass conservation is not time dependent and provides a relation between bone approach and configuration of the membrane. With this in hand, equilibrium, which is history dependent because of the biphasic nature of cartilage, can be stated as a Volterra integral equation to be solved numerically.

Following the experience of [10, 11], we question whether, besides the disadvantage of stressing the membrane, there is at least one direct mechanical advantage for swelling and pressurization in joints. We examine joints where the labrum is not responsible for constraining the fluid and, instead of having a thin film, a consistent volume is present. The parameter responsible for pressurization, according to the elastic version of Laplace's law in Eq.(13) is the membrane stiffness.

We observe numerically that the coupled mechanism of contact and pressurization is not much more fruitful than just contact. For the simulated diseased joints, though, it becomes essential that the mechanism of intra-articular self-pressurization stays functional. This can happen, of course, at the expensed of membranal elongation and stress, which might be the origin of pain. If new intra-articular fluid is injected into the cavity by the organism, the pressure would increase even further. Hence, the external load would be transmitted even more decisively via the intra-articular fluid than via direct contact.

Besides, the synovial membrane thickens when ligaments are damaged. After some time, the cartilage is damaged (Lukoschek et al. [26]). In this work's perspective it might be inferred that the thickening is not the cause of articular disorders, but a late attempt of saving the cartilage by increasing the whole mechanism stiffness. Both effusion and membrane thickening are rather a sign than a self-standing problem.

The proven synovial membrane alteration during the progression of OA has been recently analyzed both from the viewpoint of biochemical pathways and mechanical measurements at the nanoscale (e.g. see Remst et al. [37], Dai et al. [8]). The question that we pose here, i.e. the cause-effect relation between synovitis and OA, remains open and we try to enrich the discussion via a mechanical insight of the interplay between the cartilage, synovium and synovial fluid.

Further work can be done for studying lubrication inside the contact and investigating the dependence of friction on high fluid pressure at the border of the contact. This would require solving a problem of hydraulic fracture as for instance in [52, 53, 7], where the injection pressure and flow far from the crack tip is dictated by the properties of the membrane. Moreover, thanks to novel data on collagen mechanical response, the collagen network reinforcing the cartilage and lining the synovial membrane could be modeled in the framework of multiscale statistical mechanics as in Vitucci et al. [48].

In this first study, we have tackled only the 2D problem. Nevertheless, it would be interesting to extend our model to the third dimension. In such a case, indeed, according to Young-Laplace equation, the intra-articular pressure is predicted to be higher, given that both curvatures are nonzero. Whereas we do not expect qualitative differences, the confining effect could result enhanced and its quantification will be considered elsewhere. Even though the present model can be complicated with more realistic geometries, synovial fluid flow and synovium constitutive assumptions, it represents a first contribution towards a more synergistic biomechanical understanding of articular joints.

Acknowledgements

G. Vitucci is supported by the POR Puglia FESR-FSE project REFIN A1004.22; D. De Tommasi by the Italian Prin Project 2017-J4EAYB; G. Mishuris by the Visiting Professorship September 2022 of Politecnico di Bari. GM is also thankful to the Royal Society for the Wolfson Research Merit Award and EU Commission for support via MSCA RISE project EffectFact.

References

[1] Ivan Argatov and Gennady Mishuris. Elliptical contact of thin biphasic cartilage layers: Exact solution for monotonic loading. *Journal of biomechanics*, 44(4):759–761, 2011.

[2] Ivan Argatov and Gennady Mishuris. Contact mechanics of articular cartilage layers. *Asymptotic models. Springer*, 2015.

[3] G A Ateshian, W M Lai, W B Zhu, and VC Mow. An asymptotic solution for the contact of two biphasic cartilage layers. *Journal of biomechanics*, 27(11):1347–1360, 1994.

[4] D Bigoni, SK Serkov, M Valentini, and AB Movchan. Asymptotic models of dilute composites with imperfectly bonded inclusions. *International journal of solids and structures*, 35(24): 3239–3258, 1998.

[5] Federica Boschetti, Giancarlo Pennati, Francesca Gervaso, Giuseppe M Peretti, and Gabriele Dubini. Biomechanical properties of human articular cartilage under compressive loads. *Biorheology*, 41(3-4):159–166, 2004.

[6] Jeremy L Coleman, Margaret R Widmyer, Holly A Leddy, Gangadhar M Utturkar, Charles E Spritzer, Claude T Moorman III, Farshid Guilak, and Louis E DeFrate. Diurnal variations in articular cartilage thickness and strain in the human knee. *Journal of biomechanics*, 46(3):541–547, 2013.

[7] Gaspare Da Fies, Daniel Peck, Martin Dutko, and Gennady Mishuris. A temporal averaging–based approach to toughness homogenisation in heterogeneous material. *Mathematics and Mechanics of Solids*, page 10812865221117553, 2022.

[8] Shouqian Dai, Ting Liang, Tadashi Fujii, Shuangjun He, Fan Zhang, Huaye Jiang, Bo Liu, Xiu Shi, Zongping Luo, and Huilin Yang. Increased elastic modulus of the synovial membrane in a rat aclt model of osteoarthritis revealed by atomic force microscopy. *Brazilian Journal of Medical and Biological Research*, 53, 2020.

[9] H Fahrer, HU Rentsch, NJ Gerber, Ch Beyeler, Ch W Hess, and B Grunig. Knee effusion and reflex inhibition of the quadriceps. a bar to effective retraining. *Bone & Joint Journal*, 70(4):635–638, 1988.

[10] SJ Ferguson, JT Bryant, R Ganz, and K Ito. The acetabular labrum seal: a poroelastic finite element model. *Clinical Biomechanics*, 15(6):463–468, 2000.

[11] SJ Ferguson, JT Bryant, R Ganz, and K Ito. The influence of the acetabular labrum on hip joint cartilage consolidation: a poroelastic finite element model. *Journal of biomechanics*, 33 (8):953–960, 2000.

[12] SJ Ferguson, John Timothy Bryant, R Ganz, and K Ito. An in vitro investigation of the acetabular labral seal in hip joint mechanics. *Journal of biomechanics*, 36(2):171–178, 2003.

[13] Pierre Geborek, Ulrich Moritz, and FA Wollheim. Joint capsular stiffness in knee arthritis. relationship to intraarticular volume, hydrostatic pressures, and extensor muscle function. *The Journal of rheumatology*, 16(10):1351–1358, 1989.

[14] Hans Gregersen, GS Kassab, and YC Fung. Determination of membrane tension during balloon distension of intestine. *MCB-TECH SCIENCE PRESS-*, 1:191–200, 2004.

[15] Andreas Halder, Ines Kutzner, Friedmar Graichen, Bernd Heinlein, Alexander Beier, and Georg Bergmann. Influence of limb alignment on mediolateral loading in total knee replacement: in vivo measurements in five patients. *JBJS*, 94(11):1023–1029, 2012.

[16] Corinne R Henak, Benjamin J Ellis, Michael D Harris, Andrew E Anderson, Christopher L Peters, and Jeffrey A Weiss. Role of the acetabular labrum in load support across the hip joint. *Journal of biomechanics*, 44(12):2201–2206, 2011.

[17] W Herzog, S Diet, E Suter, P Mayzus, TR Leonard, C Müller, JZ Wu, and M Epstein. Material and functional properties of articular cartilage and patellofemoral contact mechanics in an experimental model of osteoarthritis. *Journal of Biomechanics*, 31(12):1137–1145, 1998.

[18] Jon T Hopkins, Christopher D Ingersoll, B Andrew Krause, Jeffrey E Edwards, and Mitchell L Cordova. Effect of knee joint effusion on quadriceps and soleus motoneuron pool excitability. *Medicine & Science in Sports & Exercise*, 33(1):123–126, 2001.

[19] Ali Hosseini, Samuel K Van de Velde, Michal Kozanek, Thomas J Gill, Alan J Grodzinsky, Harry E Rubash, and Guoan Li. In-vivo time-dependent articular cartilage contact behavior of the tibiofemoral joint. *Osteoarthritis and cartilage*, 18(7): 909–916, 2010.

[20] Shahid Jawed, Karl Gaffney, and David R Blake. Intra-articular pressure profile of the knee joint in a spectrum of inflammatory arthropathies. *Annals of the rheumatic diseases*, 56(11):686–689, 1997.

[21] MI Jayson and A St Dixon. Intra-articular pressure in rheumatoid arthritis of the knee. 3. pressure changes during joint use. *Annals of the rheumatic diseases*, 29(4):401, 1970.

[22] MIV Jayson and AStJ Dixon. Intra-articular pressure in rheumatoid arthritis of the knee. *Ann. Rheum. Dis*, 29:266, 1970.

[23] Anders Klarbring and AB Movchan. Asymptotic modelling of adhesive joints. *Mechanics of materials*, 28(1-4):137–145, 1998.

[24] RU Kleemann, D Krocker, A Cedraro, J Tuischer, and Georg N Duda. Altered cartilage mechanics and histology in knee osteoarthritis: relation to clinical assessment (icrs grade). *Osteoarthritis and cartilage*, 13(11):958–963, 2005.

[25] Vladimir A Kozlov, Vladimir G Maz'Ya, and Alexander B. *Asymptotic analysis of fields in multi-structures*. Oxford University Press on Demand, 1999.

[26] M Lukoschek, MB Schaffler, DB Burr, RD Boyd, and EL Radin. Synovial membrane and cartilage changes in experimental osteoarthrosis. *Journal of orthopaedic research*, 6(4):475–492, 1988.

[27] JTA Mäkelä, SK Han, W Herzog, and RK Korhonen. Very early osteoarthritis changes sensitively fluid flow properties of articular cartilage. *Journal of biomechanics*, 48(12):3369–3376, 2015.

[28] Emad Moeendarbary and Andrew R Harris. Cell mechanics: principles, practices, and prospects. *Wiley Interdisciplinary Reviews: Systems Biology and Medicine*, 6(5):371–388, 2014.

[29] Alexander B Movchan and Nataliya V Movchan. *Mathematical modelling of solids with nonregular boundaries*. CRC Press, 2020.

[30] Alexander B Movchan, Natasha V Movchan, and Chris G Poulton. *Asymptotic models of fields in dilute and densely packed composites*. World Scientific, 2002.

[31] Van C Mow, SC Kuei, W Michael Lai, and Cecil G Armstrong. Biphasic creep and stress relaxation of articular cartilage in compression: theory and experiments. *Journal of biomechanical engineering*, 102(1):73–84, 1980.

[32] DB Myers and DG Palmer. Capsular compliance and pressure-volume relationships in normal and arthritic knees. *Bone & Joint Journal*, 54(4):710–716, 1972.

[33] S Nade and PJ Newbold. Pressure-volume relationships and elastance in the knee joint of the dog. *The Journal of physiology*, 357(1):417–439, 1984.

[34] Harri E Panula, Mika M Hyttinen, Jari PA Arokoski, Teemu K Långsjö, Alpo Pelttari, Ilkka Kiviranta, and Heikki J Helminen. Articular cartilage superficial zone collagen birefringence reduced and cartilage thickness increased before surface fibrillation in experimental osteoarthritis. *Annals of the rheumatic diseases*, 57(4):237–245, 1998.

[35] Abby E Peters, Riaz Akhtar, Eithne J Comerford, and Karl T Bates. The effect of ageing and osteoarthritis on the mechanical properties of cartilage and bone in the human knee joint. *Scientific reports*, 8(1):1–13, 2018.

[36] JR Ralphs and M Benjamin. The joint capsule: structure, composition, ageing and disease. *Journal of anatomy*, 184(Pt 3): 503, 1994.

[37] Dennis FG Remst, Esmeralda N Blaney Davidson, and Peter M van der Kraan. Unravelling osteoarthritis-related synovial fibrosis: a step closer to solving joint stiffness. *Rheumatology*, 54(11): 1954–1963, 2015.

[38] Derek James Rutherford. Intra-articular pressures and joint mechanics: Should we pay attention to effusion in knee osteoarthritis? *Medical hypotheses*, 83(3):292–295, 2014.

[39] N Schwarz, M Leixnering, R Hopf, and S Jantsch. Pressure-volume ratio in human cadaver hip joints. *Archives of orthopaedic and traumatic surgery*, 107(5):322–325, 1988.

[40] Lori A Setton, Dawn M Elliott, and Van C Mow. Altered mechanics of cartilage with osteoarthritis: human osteoarthritis and an experimental model of joint degeneration. *Osteoarthritis and cartilage*, 7(1):2–14, 1999.

[41] Malcolm D Smith and Mihir D Wechalekar. The synovium. 2014.

[42] JD Spencer, KC Hayes, and Ian J Alexander. Knee joint effusion and quadriceps reflex inhibition in man. *Archives of physical medicine and rehabilitation*, 65(4):171–177, 1984.

[43] Jocelyn N Todd, Travis G Maak, Gerard A Ateshian, Steve A Maas, and Jeffrey A Weiss. Hip chondrolabral mechanics during activities of daily living: Role of the labrum and interstitial fluid pressurization. *Journal of Biomechanics*.

[44] Michael R Torry, Michael J Decker, Randall W Viola, Dennis D O'Connor, and J Richard Steadman. Intra-articular knee joint effusion induces quadriceps avoidance gait patterns1. *Clinical Biomechanics*, 15(3):147–159, 2000.

[45] MJ Viitanen, AM Wilson, HP McGuigan, KD Rogers, and SA May. Effect of foot balance on the intra-articular pressure in the distal interphalangeal joint in vitro. *Equine veterinary journal*, 35(2):184–189, 2003.

[46] Gennaro Vitucci and Gennady Mishuris. Three-dimensional contact of transversely isotropic transversely homogeneous cartilage layers: A closed-form solution. *European Journal of Mechanics-A/Solids*, 65:195–204, 2017.

[47] Gennaro Vitucci, Ivan Argatov, and Gennady Mishuris. An asymptotic model for the deformation of a transversely isotropic, transversely homogeneous biphasic cartilage layer. *Mathematical Methods in the Applied Sciences*, 40(9):3333–3347, 2017.

[48] Gennaro Vitucci, Domenico De Tommasi, Giuseppe Puglisi, and Francesco Trentadue. A predictive microstructure-based approach for the anisotropic damage, residual stretches and hysteresis in biodegradable sutures. *arXiv preprint arXiv:2206.00345*, 2022.

[49] Sarah Catherine Walpole, David Prieto-Merino, Phil Edwards, John Cleland, Gretchen Stevens, and Ian Roberts. The weight of nations: an estimation of adult human biomass. *BMC public health*, 12(1):1–6, 2012.

[50] UGK Wegst and MF Ashby. The mechanical efficiency of natural materials. *Philosophical Magazine*, 84(21):2167–2186, 2004.

[51] Frederick W Werner, David C Ayers, Lorin P Maletsky, and Paul J Rullkoetter. The effect of valgus/varus malalignment on load distribution in total knee replacements. *Journal of biomechanics*, 38(2):349–355, 2005.

[52] Michal Wrobel and Gennady Mishuris. Hydraulic fracture revisited: Particle velocity based simulation. *International Journal of Engineering Science*, 94:23–58, 2015.

[53] Michal Wrobel, Gennady Mishuris, and Andrea Piccolroaz. Energy release rate in hydraulic fracture: can we neglect an impact of the hydraulically induced shear stress? *International Journal of Engineering Science*, 111:28–51, 2017.

[54] Chi-Hung Yen, Hon-Bong Leung, and Paul Yun-Tin Tse. Effects of hip joint position and intra-capsular volume on hip joint intra-capsular pressure: a human cadaveric model. *Journal of orthopaedic surgery and research*, 4(1):8, 2009.

Appendix A. Derivation of the analytical results in Sec.2.1

Firstly, we assume that the auxiliary function

$$p(x,t) = \mathcal{K}[P(x,\cdot)](t) \tag{A.1}$$

satisfies a priori the boundary conditions Eqs.(2)-(3) with $P_f = 0$ as

$$p(x,t) = \bar{p}\left(a^2(t) - x^2\right)^2. \tag{A.2}$$

The substitution the latter into Eq.(1) and equating the coefficients which multiply the same degree of x allows one to determine

$$\bar{p} = \frac{m}{24R}, \qquad \delta(t) = \frac{a^2(t)}{6R}. \tag{A.3}$$

Let us multiply Eq.(1) by $x^2/2$ and integrate it over the contact domain

$$\int_{-a(t)}^{a(t)} \frac{x^2}{2}\frac{\partial^2 p(x,t)}{\partial x^2}\,\mathrm{d}x = m\int_{-a(t)}^{a(t)} \frac{x^2}{2}\left(\frac{x^2}{2R} - \delta(t)\right)\mathrm{d}x. \tag{A.4}$$

The contact displacement scales with the square of the contact width, a common feature with the 3D contact as derived in [46]. If one integrates the left-hand side by parts twice, this becomes

$$\int_{-a(t)}^{a(t)} p(x,t)\,\mathrm{d}x = \mathcal{K}\left[\int_{-a(t)}^{a(t)} P(x,t)\,\mathrm{d}x\right](t) = \frac{1}{2}\mathcal{K}[F_c](t), \tag{A.5}$$

via enforcing Eq.(3) and (2). By substituting Eq.(A.3) into the right-hand side of Eq.(A.4) and integrating explicitly, finally the time-dependent half-width of the contact domain is found to be

$$a(t) = \left(\frac{45R}{2m}\mathcal{K}[f](t)\right)^{1/5}. \tag{A.6}$$

It is perhaps worth noticing that in the case of 3D contact, due to one more dimension, the exponent of the left-hand side is one sixth. Hence, according to Eqs.(A.1) and (A.2), one also has the solution in terms of contact pressure

$$P(x,t) = \frac{m}{24R}\mathcal{K}^{-1}\left[\left(a^2(\cdot) - x^2\right)^2\right](t). \tag{A.7}$$

Nonzero pressure at the boundary. Let us consider the the same problem as above, but let us change the boundary conditions of P from to

$$P = P_f(t), \qquad \frac{\partial P}{\partial x} = 0 \qquad \text{for} \quad x = \pm a(t). \tag{A.8}$$

It means assigning a border value to the contact pressure while preserving its flatness, due to the peculiar surface stresses of biphasic layers as discussed in [46]. In this case the guess on $p = \mathcal{K}P$ becomes

$$p(x,t) = \frac{m}{24R}\left(a^2(t) - x^2\right)^2 + P_f. \tag{A.9}$$

See that the imposed P_f has no effect in terms of the contact displacement δ versus a relation, as the second derivative of P_f, entering the unchanged Eq.(1) is nil. By applying the same integration by parts as Eq.(A.4), one obtains now the equation for finding the half-width of the contact area

$$\frac{m}{45R}a^5(t) + \mathcal{K}[aP_f](t) - \frac{1}{2}\mathcal{K}[F_c](t) = 0, \tag{A.10}$$

that is an integral quintic in a that can not be solved but numerically, in contrast to the case of zero border pressure in Eq.(8). Once $a(t)$ is known, the problem is considered to be solved also in terms of pressure field by inverting Eq.(A.9) into

$$P(x,t) = P_f(t) + \frac{m}{24R}\mathcal{K}^{-1}\left[\left(a^2(\cdot) - x^2\right)^2\right](t). \tag{A.11}$$

Appendix B. Derivation of mass balance and equilibrium in Sec.2.3

The unknown δ can be expressed as function of $a^2/(6R)$ via Eq.(6), therefore

$$r(t)\sin\theta(t) = \frac{d^2}{2R} - \frac{a(t)^2}{6R}. \tag{B.1}$$

The unknowns θ, r and b are also interdependent (see Fig.1):

$$b(t) = (1 - \cos\theta(t))\,r(t). \tag{B.2}$$

Similarly as in Eq.(14) this allows computing the fluid volume as

$$A(\theta) = d\frac{d^2 - a^2(\theta)}{6R} + \frac{r^2(\theta)}{2}\left(\theta - \sin\theta\cos\theta\right). \tag{B.3}$$

The equilibrium of the membrane gives one more relation

$$P_f(t)r(t) = T(t) \qquad \forall t, \tag{B.4}$$

which is equivalent to Young-Laplace equation in 2D. Lastly, by integrating the constitutive equation of the membrane Eq.(12) in the present case of circular configuration, one obtains

$$T(t) = T_0 + S(l(t) - l_0)), \tag{B.5}$$

where the subscript 0 refers to a known configuration at the time $t = t_0$. l is the membrane length

$$l(t) = r(t)\theta(t) = \left(\frac{d^2}{2R} - \delta(t)\right)\frac{\theta(t)}{\sin\theta(t)}. \tag{B.6}$$

Summarizing, we have two main equations, mass conservation and vertical equilibrium Eqs.(B.3) and (19), plus a set of five additional relations which allow to reduce the problem to the search of two functions of time, e.g. $a(t)$ and $\theta(t)$. Namely, by simple substitutions:

$$\frac{d}{6R}(d^2 - a^2) + \left(\theta - \frac{\sin 2\theta}{2}\right)\frac{r^2(a,\theta)}{2} - A_0 = 0;$$
$$\frac{m}{45R}\mathcal{K}^{-1}\left[a^5\right](t) + \left(\frac{d}{r(a,\theta)} - \cos\theta\right)T(a,\theta) - \frac{F(t)}{2} = 0. \tag{B.7}$$

Reduction to one unknown. In order to reduce the number of unknowns, one can solve the first of Eq.(B.7) for $a = a(\theta)$. Introducing, for instance, the auxiliary function

$$\Phi(\theta) = \frac{\theta - \frac{\sin 2\theta}{2}}{2\sin^2\theta}, \tag{B.8}$$

the mass conservation becomes a quadratic in δ:

$$\Phi(\theta)\delta^2 - \left(d + \Phi(\theta)\frac{d^2}{R}\right)\delta - \left(A_0 - \frac{d^3}{6R} - \Phi(\theta)\frac{d^4}{4R^2}\right) = 0. \tag{B.9}$$

It's solution, coherent with the choice of

$$\theta \in [0;\pi], \tag{B.10}$$

is:

$$\delta(\theta) = \frac{a^2(\theta)}{6R} = \frac{d}{2\Phi} + \frac{d^2}{2R} - \sqrt{\left(\frac{d}{2\Phi} + \frac{d^2}{2R}\right)^2 + \frac{1}{\Phi}\left(A_0 - \frac{d^3}{6R} - \Phi\frac{d^4}{4R^2}\right)}, \tag{B.11}$$

which simplifies into $\delta = \frac{d^2}{6R} - \frac{A_0}{d}$ for $\theta = 0$.

Now, with $a(\theta)$ in one hand, the second equation in Eq.(B.7), i.e. the equilibrium balance, reduces to the search for θ from

$$\frac{m}{45R}\mathcal{K}^{-1}\left[a^5(\theta(\cdot))\right](t) + \left(\frac{d}{r(\theta(t))} - \cos\theta(t)\right)T(\theta(t)) = \frac{F(t)}{2} \tag{B.12}$$

at every time t.

Reduction to ordinary differential equation. In order to numerically solve Eq.(B.12), we transform it into an ordinary differential equation as follows. Let us introduce the auxiliary function

$$\beta(\theta,t) = \left(\frac{d}{r(\theta(t))} - \cos\theta(t)\right)T(\theta(t)). \tag{B.13}$$

By applying the operator $\mathcal{K}$ one can rewrite Eq.(B.12) as

$$\frac{m}{45R}a^5(\theta,t) = \frac{1}{2}\mathcal{K}[F(\cdot) - 2\beta(\theta,\cdot)](t). \tag{B.14}$$

By looking at the definition Eq.(4) and using the chain rule, the equation above can be differentiated with respect to time t and rearranged as

$$\frac{\mathrm{d}\theta}{\mathrm{d}t} = \frac{1}{2\tau}\frac{F - 2\beta + \tau\frac{\mathrm{d}F}{\mathrm{d}t}}{\frac{\partial}{\partial\theta}\left(\frac{m}{45R}a^5 + \beta\right)}, \quad \theta(0) = \theta_0. \tag{B.15}$$

This is an ordinary differential equation in θ which can be solved numerically by standard procedures. The partial derivatives of a and β with respect to θ on the right-hand side can be analytically found by differentiation of Eqs.(B.1)–(B.6), whereas $F(t)$ is supposed to be known.